



**HAL**  
open science

# Investigation of the Mechanical Properties of Flax Cell Walls during Plant Development: The Relation between Performance and Cell Wall Structure

Camille Goudenhooft, David Siniscalco, Olivier Arnould, Alain Bourmaud, Olivier Sire, Tatyana Gorshkova, Christophe Baley

## ► To cite this version:

Camille Goudenhooft, David Siniscalco, Olivier Arnould, Alain Bourmaud, Olivier Sire, et al.. Investigation of the Mechanical Properties of Flax Cell Walls during Plant Development: The Relation between Performance and Cell Wall Structure. *Fibers*, 2018, 6 (1), pp.6. 10.3390/fib6010006 . hal-01690075

**HAL Id: hal-01690075**

**<https://hal.science/hal-01690075v1>**




Submitted on 22 Jan 2018

**HAL** is a multi-disciplinary open access archive for the deposit and dissemination of scientific research documents, whether they are published or not. The documents may come from teaching and research institutions in France or abroad, or from public or private research centers.

L'archive ouverte pluridisciplinaire **HAL**, est destinée au dépôt et à la diffusion de documents scientifiques de niveau recherche, publiés ou non, émanant des établissements d'enseignement et de recherche français ou étrangers, des laboratoires publics ou privés.

Communication

# Investigation of the Mechanical Properties of Flax Cell Walls during Plant Development: The Relation between Performance and Cell Wall Structure

Camille Goudenhoofft <sup>1,\*</sup> , David Siniscalco <sup>1</sup>, Olivier Arnould <sup>2</sup> , Alain Bourmaud <sup>1</sup>, Olivier Sire <sup>3</sup>, Tatyana Gorshkova <sup>4</sup>  and Christophe Baley <sup>1</sup>

<sup>1</sup> Institut de Recherche Dupuy de Lôme (IRDL), Université Européenne Bretagne, CNRS FRE 3744, 56321 Lorient, France; david.siniscalco@univ-ubs.fr (D.S.); alain.bourmaud@univ-ubs.fr (A.B.); christophe.baley@univ-ubs.fr (C.B.)

<sup>2</sup> Laboratoire de Mécanique et Génie Civil (LMGC), Université de Montpellier, CNRS UMR 5508, 34095 Montpellier, France; olivier.arnould@umontpellier.fr

<sup>3</sup> Institut de Recherche Dupuy de Lôme (IRDL), Université Européenne Bretagne, CNRS FRE 3744, 56017 Vannes, France; olivier.sire@univ-ubs.fr

<sup>4</sup> Kazan Institute of Biochemistry and Biophysics (KIBB), Kazan Scientific Centre, Russian Academy of Sciences, 420111 Kazan, Russia; gorshkova@kibb.knc.ru

\* Correspondence: camille.goudenhoofft@univ-ubs.fr; Tel.: +33-297-874-518

Received: 22 December 2017; Accepted: 11 January 2018; Published: 17 January 2018

**Abstract:** The development of flax (*Linum usitatissimum* L.) fibers was studied to obtain better insight on the progression of their high mechanical performances during plant growth. Fibers at two steps of plant development were studied, namely the end of the fast growth period and at plant maturity, each time at three plant heights. The indentation modulus of the fiber cell wall was characterized by atomic force microscopy (AFM) using peak-force quantitative nano-mechanical property mapping (PF-QNM). Changes in the cell wall modulus with the cell wall thickening were highlighted. For growing plants, fibers from top and middle heights show a loose inner Gn layer with a lower indentation modulus than mature fibers, which exhibit thickened homogeneous cell walls made only of a G layer. The influence of these changes in the fiber cell wall on the mechanical performances of extracted elementary fibers was also emphasized by tensile tests. In addition, Raman spectra were recorded on samples from both growing and mature plants. The results suggest that, for the fiber cell wall, the cellulose contribution increases with fiber maturity, leading to a greater cell wall modulus of flax fibers.

**Keywords:** fiber crops; flax fibers; cell wall; thickening; AFM (Atomic Force Microscopy); tensile test; Raman spectroscopy

## 1. Introduction

For centuries, flax (*Linum usitatissimum* L.) has been cultivated as a fiber crop in order to produce textiles [1]. Fiber flax is not only used in the clothing industry, as its technical fibers have also been used as reinforcement for composite materials since the 1930s [2]. Flax technical fibers are composed of elementary fibers, whose average performances reach a longitudinal Young's modulus of  $52.47 \pm 8.57$  GPa, a tensile strength of  $945 \pm 200$  MPa, and a strain at break of  $2.07 \pm 0.45\%$ ; furthermore, their average specific mechanical properties were proven to compete with those of glass fibers [3].

In addition, flax is also a unique model for studying cell growth. Indeed, its fibers can reach a length of several tens of millimeters [4]. Moreover, the cell wall thickness in fibers is impressively high, as it can reach more than 10  $\mu\text{m}$ , while most cell walls are less than a few microns thick [5].

These geometrical singularities make flax a very interesting reference regarding cell development and elongation [4].

As in plant cells, the complex mechanism of fiber development can be simplified into two main steps: elongation and thickening [6]. Their elongation appears only at the top part of the stem, above a region called “snap point,” also identified as the point where a change in effort is required to easily break the stem by hand [7]. Crop growth takes place over 50–70 days and finalizes during flowering [8]. Moreover, for flax, the crop growth is itself divided into different phases. First, fast growth occurs about a month after sowing, over a 15-day period during which the stem elongates several centimeters per day. The stem grows from 10–20 to 80 cm during fast growth. Once fast growth slows down, the stem keeps growing upon floral budding, i.e., until the plant is about 60–70 days old. The intensive thickening of the cell walls lasts about 60 days and takes place mainly below the snap point [7]. More precisely, the thick cell wall of fibers, called either the S2 or G layer, with a gelatinous appearance due to its gel-like matrix similar to tension wood fibers [9], is progressively formed from the conversion of an inner sublayer known as Gn layer [5]. Later on, the G layer increases in thickness until complete conversion of Gn layer which leads to a more homogeneous and compacted layer, over cell maturation [5]. Finally, fiber maturity is reached about 120 days after sowing and plants are pulled out to undergo a dew retting process [8].

Even though the course of fiber development is known, the consequences in terms of mechanical properties over plant growth have yet to be characterized. How does the cell wall development lead to the impressive geometrical and mechanical properties of flax fibers? This study investigates the characteristics of cell wall properties of flax fibers during plant development. Two important stages of the development were studied: finalization of crop growth (60 days after sowing) and maturity (120 days after sowing). Moreover, three height positions in the stem were chosen for the investigation, namely top, bottom, and middle parts of the stem. The evolution of the local indentation modulus of fiber cell wall layers was characterized by peak-force quantitative nano-mechanical property mapping (PF-QNM), a powerful tool for imaging possible gradients in stiffness of wood and other plant cell walls [10,11]. Mechanical properties of extracted single fibers over plant growth were also estimated by tensile tests, a reliable method to evaluate the average apparent tensile properties of flax fibers [3]. Finally, cellulose contribution was investigated over plant development using confocal Raman spectroscopy [12–14], in order to correlate the indentation modulus and the fiber structure.

## 2. Materials and Methods

### 2.1. Plant Material and Culture Conditions

Flax seeds (Eden variety) were provided by Terre de Lin (a French agricultural cooperative based in Normandy). Sowing was done at the end of March 2016 in Lorient (France). A seeding density of 1800 plants/m<sup>2</sup> was used, which corresponds to the conventional density for flax cultivation [8]. A first batch of stems was pulled out 60 days after sowing (60 days batch), during the finalization of fast growth period of plant development. The second batch was pulled out at maturity, 120 days after sowing (120 days batch).

### 2.2. Sample Preparation Prior Atomic Force Microscopy (AFM) Peak Force Quantitative Nano-Mechanical (QNM) Measurements

For each batch, samples of 1 cm long were cut from stems using a razor blade, immediately after plants being pulled out. Three samples per stem, using a single stem per sampling date, were taken: the bottom one around 2 cm above cotyledons, one sample from middle height, and one at the top around 2 cm below the snap point (60 days batch) or below the first stem ramification (120 days batch). Samples were immediately placed in an ethanol/deionized water solution (1/1) for several days and stored at 4 °C.

Flax stem samples were then treated with a series of ethanol/deionized water solutions progressively enriched in ethanol (50%, 75%, 90%, and 100%). Dehydrated samples can so be embedded in a mixture of increasing ratios of London Resin (LR)-White acrylic resin/ethanol (25%, 50%, 75%, and 100% resin). Final resin polymerization was performed in an oven (60 °C overnight).

Embedded samples were finally machined into a pyramidal shape to reduce their cross-section and cut using an ultramicrotome (Leica Ultracut R) equipped with diamond knives (Diatome Histo and Ultra AFM). It is well-known that the procedure of sample preparation before embedding as well as the embedding medium itself can modify cell wall properties [15,16] but not that much for LR-White or other acrylic-like resin [17,18], especially with the reduction in time at each step of the embedding process used in the present study. The authors thus consider that stiffness values are not significantly affected by the embedding resin in the present study. Moreover, it is mandatory for the present study to use embedded samples prior to AFM peak-force QNM measurements. First of all, the mentioned preparation reduces the artifacts coming from the sample surface roughness or border effect in order to provide reliable contact moduli [10]. In addition, in order to maintain the cell wall structure and avoid G layer detachment and collapse due to stress release during the sample surface preparation, namely during the cutting process, it is necessary to fill the lumen of fibers by embedding [19]. Nevertheless, the local indentation modulus does not correspond to in planta values but to dry ones and cannot be assimilated to absolute values of the longitudinal cell wall stiffness [20]. However, relative values can be taken into account for suitable comparisons.

### 2.3. AFM Peak Force QNM Measurements

AFM measurements were performed with a Multimode AFM instrument (Bruker Corporation, Santa Barbara, CA, USA). PF-QNM imaging mode with a RTESPA-525 (Bruker) probe with a spring constant of 139 N/m and a tip radius between 15 and 35 nm were used. The tip and cantilever of the probe were calibrated as detailed in Arnould et al. [11]. A scan rate of 8  $\mu\text{m/s}$  and a maximum load of 200 nN were used for all the measurements. Nanoindentation measurements of the indentation modulus of the embedding resin and at some location in cell wall G layers of each sample were also done and serve as a control for AFM measurements [11].

### 2.4. Tensile Tests Performed on Extracted Elementary Fibers

For each batch, samples of 10 cm long were cut from the middle part of the stems and immediately placed in an ethanol/deionized water solution (1/1) for several days at 4 °C. Then, elementary fibers were extracted manually after immersion of the samples in 1/1-ethanol/water for at least 24 h to facilitate the extraction. Fiber strain at break, strength at break, and tangent Young's modulus were determined from tensile tests on elementary fibers (NF T25-501-2). For each tested batch, the fiber testing experiment was performed as detailed in Goudenhooff et al. [21]. To consider the real cell wall contribution, i.e., to take the presence of the lumen into account, the mean effective cell wall filling ratio of fibers from mid-stem was measured optically on the stem cross-section.

### 2.5. Raman Spectroscopy

Raman spectra were obtained using a confocal Raman system (InduRam, Jobin-Yvon, Palaiseau, France). The system consists of a 785 nm laser source with a 2  $\mu\text{m}$  laser spot and a BX41 microscope (Olympus) with an objective of magnitude 50 (NA 0.50). All spectra were obtained on machined LR-White embedded stem samples (previously used for AFM measurements) by averaging 60 measurements (2 s integration time) in the 300–1800  $\text{cm}^{-1}$  range. Pure resin spectra were also collected to numerically remove its contribution from fibers spectra when necessary.

## 2.6. Statistical Analysis

Multivariate statistical analyses were performed using Raman spectra. LDA (Linear Discriminant Analysis) was used to discriminate age groups and to correlate the indentation modulus with Raman spectra. All analyses were performed with The Unscrambler (Camo, Oslo, Norway) software.

## 3. Results and Discussion

### 3.1. AFM Peak Force QNM Measurements

To monitor the fiber indentation modulus along the stem during plant growth, bottom, middle, and top parts of a single stem were analyzed. Figure 1 shows AFM images from three samples of a single 60-day old plant, where fibers during thickening of the cell wall are visible.

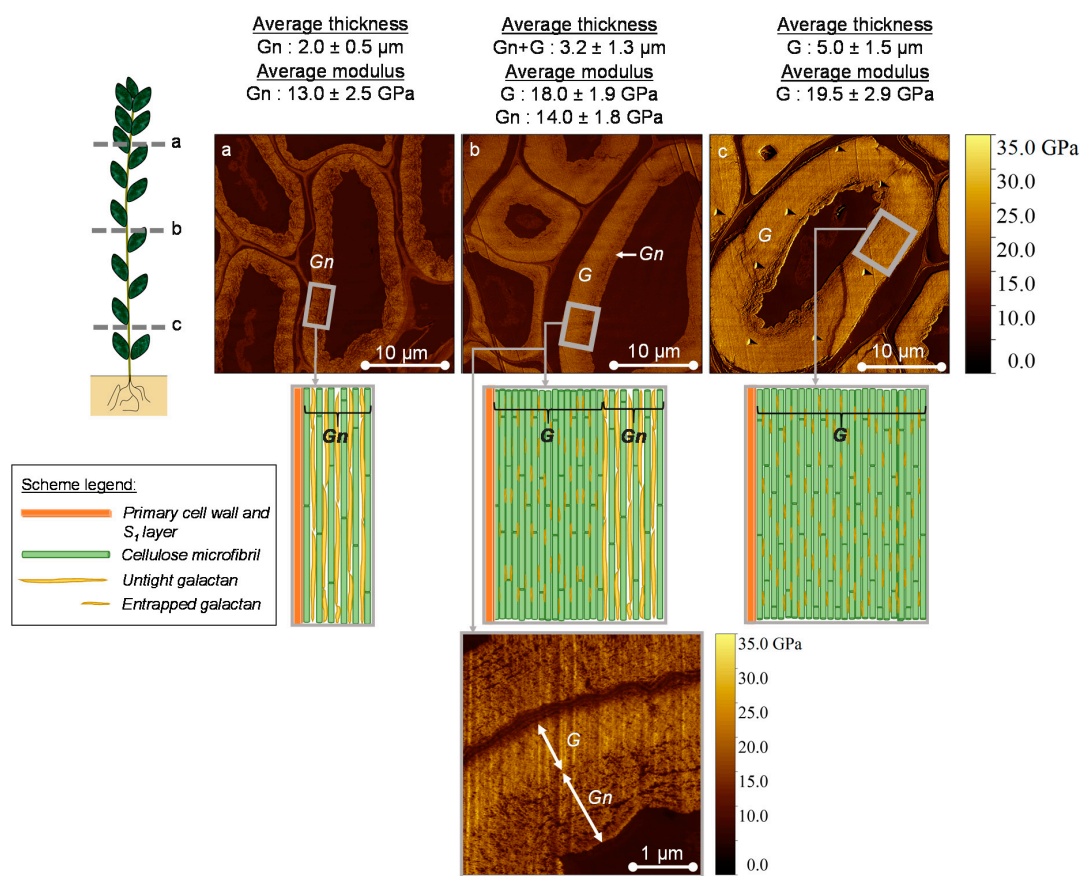


**Figure 1.** Atomic force microscopy (AFM) peak-force quantitative nano-mechanical (PF-QNM) mapping of the indentation modulus of developing flax fibers below snap point at top (a), middle (b), and bottom (c) parts of the stem at the end of fast growth period (60 days after sowing). The Gn layer visible at the top and middle parts is characterized by a low modulus and loose portions (a,b). These properties of the Gn layer are attributed to cellulose microfibrils separated by long galactan chains present in nascent rhamnogalacturonan-I [5]. The G layer at the middle and bottom parts has a higher modulus and is more homogeneous (b,c). The G layer is assumed to be characterized by the entrapped rhamnogalacturonan-I with partially trimmed off galactan side chains and packed due to lateral interactions microfibrils [5]. Indent triangular prints on (c) come from preliminary nano-indentation calibration. Scheme inspired from Mikshina et al. [5].

The top part of the stem is characterized by fibers with thinner cell walls (Figure 1a). Their low indentation modulus ( $13.0 \pm 2.5 \text{ GPa}$ ) is attributed to predominant loose portions of the Gn layer, whereas the G layer is almost invisible. For this newly formed layer in the thickened cell wall, the loose

portions of the Gn layer (schematized on Figure 1) might result from long galactan chains present in the nascent version of tissue- and stage-specific rhamnogalacturonan-I. The galactan chains separate cellulose microfibrils, leading to their loose packing [5].

At mid-stem (Figure 1b), gradients in terms of local indentation modulus are visible on fiber cell walls, with averages values from  $14.0 \pm 1.8$  GPa for the Gn layer to  $18.0 \pm 1.9$  GPa for the G layer [11]. The looser appearance of the Gn layer and its lower indentation modulus compared to the G layer argue for a mechanism of aggregation of cellulose microfibrils and entrapment of the matrix material, during the maturation of the cell wall from Gn to G layer. This maturation could induce a change in the cell wall structure that leads to changes in the mechanical properties, in parallel to the induction of the tensile stress [9,22]. However, when the fibers from the bottom part of the plant are considered (Figure 1c), although a thin Gn layer is still visible at this stage of growth, the major portion of the thickened cell wall is much more homogeneous and gives higher mechanical properties (an indentation modulus of  $19.5 \pm 2.9$  GPa). In fact, the G layer increased in thickness until the almost complete conversion of the Gn layer, leading to a more homogeneous and compacted layer [5]. Visualization of the differences in mechanical properties between distinct cell wall layers in developing flax fibers clearly matches the previously published pictures obtained by immunolabeling with LM5 antibody [23,24], with LM5 specifically recognizing beta-1,4-galactans [25]. Based on these works, the Gn layer has a much higher density of labeling than the G layer, indicating that modification of the rhamnogalacturonan-I side chains is important for the developing of cell wall mechanical properties. Finally, from a mechanical and structural point of view, at a given time, the growing flax plant gathers, from its top to its bottom, all developing steps of the fiber cell walls.

To evaluate the development and properties of the fiber cell wall along the stem at fiber maturity (corresponding to the conventional pulling time), additional AFM images were collected. Figure 2 shows that fibers from all stem locations exhibit thick cell walls with homogeneous indentation moduli within single fibers, but also between fibers ( $17.3 \pm 1.7$  GPa for the top,  $18.4 \pm 1.3$  GPa for the middle, and  $17.7 \pm 1.4$  GPa for the bottom fibers).

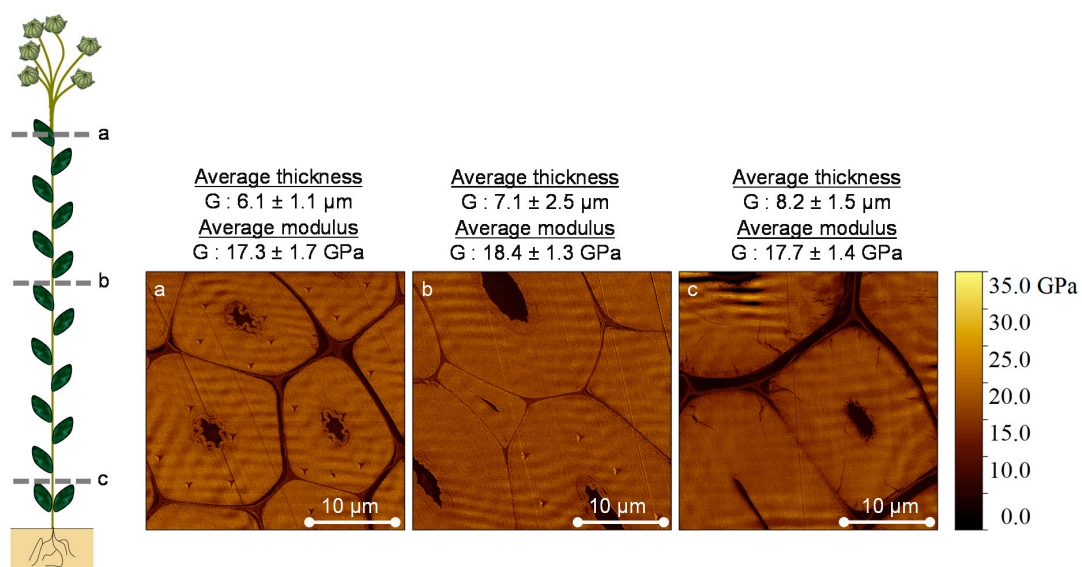


**Figure 2.** AFM PF-QNM mapping of the indentation modulus of flax fibers from mature plant (120 days after sowing) at the top (a), middle (b), and bottom (c) parts of the stem. Mature fibers are characterized by thick cell walls having a homogeneous modulus for all studied parts of the stem. Apparent waves on the map come from AFM laser interferences that lead to adhesion force artifacts and were not taken into account in the statistical analysis.

The loose Gn layer is still visible in some fibers, mainly in the top location (Figure 2a). This unfinished Gn layer transformation, representing only a negligible part of the whole fiber section, could be attributed to a lack of time to reach fiber maturity at the top level, as these fibers were the latest to be formed. Even though strong but stable wave artifact (coming from AFM laser interferences that lead to adhesion force artifacts) is visible on every image given in Figure 2, it does not prevent the comparison of neither the changes in the fiber morphology nor the relative average indentation modulus. Finally, at maturity, fibers are well formed with thickened cell walls, i.e., small lumens. Moreover, mature fibers exhibit a high and homogeneous indentation modulus whatever their location along the stem. In addition, diversity in absolute values may exist between plants, since the materials studied are of biological origin. This may explain to a large extent why the indentation moduli of G layers in Figure 2 are sometimes slightly lower than those in Figure 1b,c.

### 3.2. Tensile Tests Performed on Extracted Elementary Fibers

In order to evaluate the influence of the Gn layer at a larger scale, mechanical properties of elementary fibers were characterized by tensile tests. Fibers from mid-stem for both 60-day-old plants and mature ones were tested, as only the former batch showed a Gn layer on AFM images. Figure 3 gives the comparison between the properties of elementary flax fibers extracted from the plants previously mentioned.

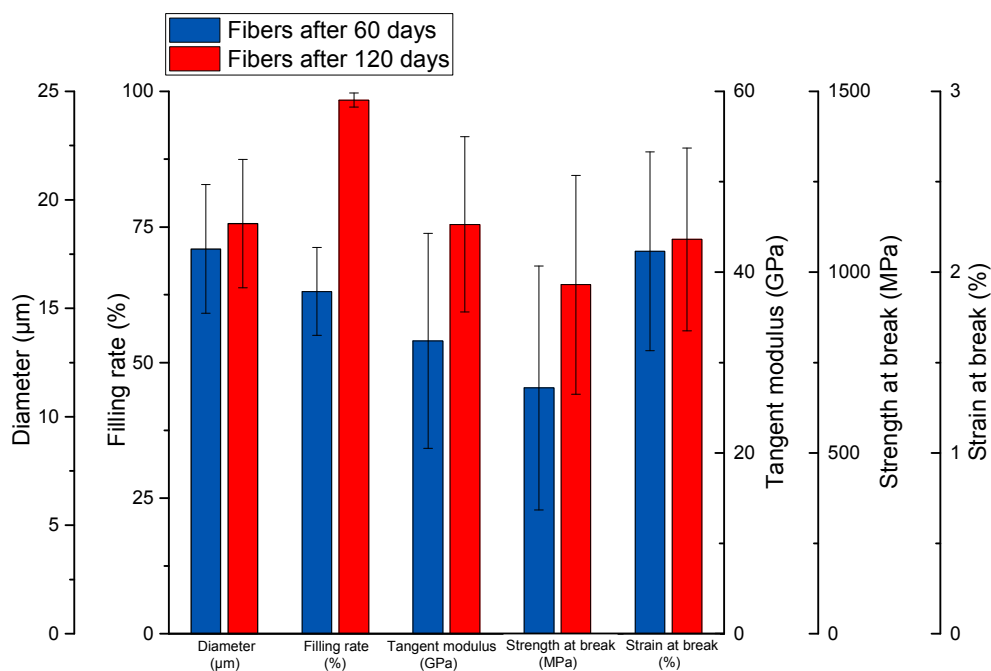


**Figure 3.** Properties of elementary flax fibers at mid-stem height and mechanical performances obtained from tensile tests performed on fibers extracted from plants of 60 days and 120 days after sowing.

For developing fibers with a filling rate of  $63.1 \pm 8.1\%$ , an average tangent Young's modulus of  $32.4 \pm 11.9$  GPa, and a strength at break of  $680 \pm 337$  MPa were estimated, whereas much higher performances were observed for mature fibers (namely, a tangent modulus of  $45.3 \pm 9.7$  GPa and a strength at break of  $965 \pm 302$  MPa). These values correspond to the whole cell wall average longitudinal Young's modulus and strength at break, as the presence of the lumen has been taken into account. However, both batches exhibit a similar strain at break, namely  $2.12 \pm 0.55\%$  for developing fibers and  $2.18 \pm 0.51\%$  for mature ones. It is important to keep in mind here that values of indentation modulus in the fiber cell wall are lower than the longitudinal tangent Young's modulus due to the anisotropic behavior of the cell wall layers [20]. In addition, the relationship between the indentation

modulus and the tensile modulus of developing fibers as well as of mature fibers is in accordance with the values given in the literature [26].

### 3.3. Raman Spectral Results

In order to highlight potential differences in terms of composition between the samples, an analysis combining Raman spectroscopy with a linear discriminant analysis was performed. In this way, the degree of plant maturity was used as a parameter, i.e., all Raman spectra from 60 day samples were used as a single batch, while 120 day samples led to spectra identified as the other batch. The LDA led to 89% of correctly discriminated spectra for the 60 days batch, while 83% of the 120 days batch was correctly discriminated. For each batch, an average Raman spectrum was computed from the correctly discriminated spectra only (Figure 4a). By comparing these average spectra from the two batches, one can notice that the same Raman lines can be identified, proving that the qualitative cell wall composition is unchanged over cell wall development.

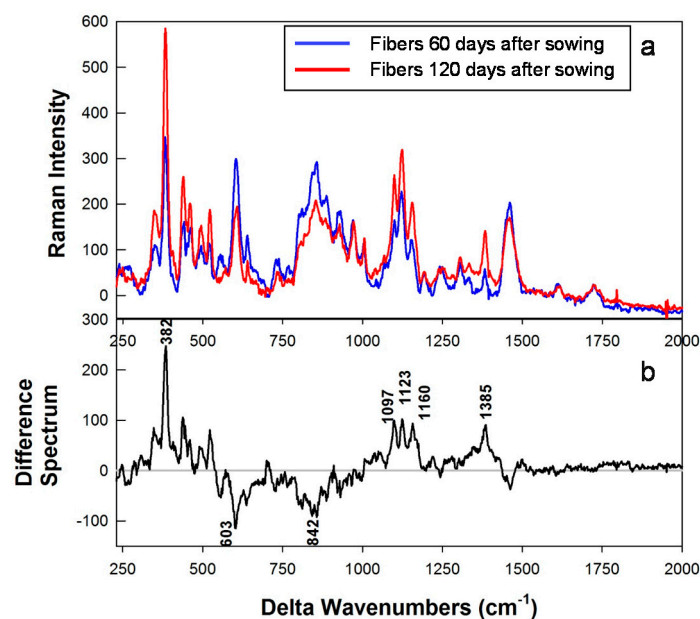


**Figure 4.** Average Raman spectra obtained from the correctly discriminated spectra of the 60 day and 120 day samples, respectively (a) and their difference spectrum (b). Raman lines  $382\text{ cm}^{-1}$ ,  $1097\text{ cm}^{-1}$ ,  $1123\text{ cm}^{-1}$ , and  $1385\text{ cm}^{-1}$  (attributed to cellulose) differentiate the two levels of flax cell wall maturity, with higher intensities for the 120 day sample. The Raman line  $842\text{ cm}^{-1}$  (attributed to galactans) decreases with fiber maturity, as does the  $603\text{ cm}^{-1}$  one (which corresponds to the embedding resin, whose content decreases as lumen size, with fiber wall thickening, decreases).

In addition, the difference spectrum of the average spectra of the two batches is also displayed (Figure 4b). From this difference spectrum, several Raman lines allow for distinguishing discriminant between the two levels of maturity. Firstly, the Raman line  $842\text{ cm}^{-1}$  decreases with fiber maturity; this line can be attributed to pectic polysaccharides such as galactans [13,27]. This decrease is in accordance with the changes in the galactan structure occurring during the transformation of the Gn layer into the G layer, previously highlighted in Figure 1, namely long galactan chains are partially trimmed off from the rhamnogalacturonan-I backbone by the action of tissue-specific galactosidase [5]. Secondly, Raman lines  $382\text{ cm}^{-1}$ ,  $1097\text{ cm}^{-1}$ ,  $1123\text{ cm}^{-1}$ , and  $1385\text{ cm}^{-1}$  also differentiate the fiber maturity. Similar wavelengths ( $379\text{ cm}^{-1}$ ,  $1095\text{ cm}^{-1}$ ,  $1120\text{ cm}^{-1}$ , and  $1379\text{ cm}^{-1}$ ) have been reported in the literature as characterizing microcrystalline cellulose [13], while  $1380\text{ cm}^{-1}$  was found to selectively characterize the G layer of poplar wood [28]. Moreover, these wavelengths were also assigned to specific vibrational modes related to molecular groups of cellulose [14]. It can be assumed that changes



in the cellulose microfibrils appear with fiber maturity; this could be linked to the increase of the microfibrils volume fraction during their aggregation (scheme in Figure 1), leading to better mechanical properties, namely a higher cell wall indentation modulus characterizing the mature fibers.

#### 4. Conclusions

PF-QNM AFM and Raman spectroscopy were combined to investigate the properties of flax fiber cell walls over plant development. The lowest indentation modulus (13–14 GPa), characterizing the Gn layer, were measured for growing fibers. However, the mature G layer exhibits a greater indentation modulus (about 18 GPa). The evolution of mechanical properties over fiber development was confirmed by tensile tests. In addition, thickened cell walls in fibers have a homogeneous morphology, as the Gn layer is completely transformed in the G layer over cell maturation. Raman spectroscopy highlights a change in cellulose over fiber thickening. Thus, for the flax fiber cell wall, changes in the mechanical properties measured by AFM could be attributed to the microfibril aggregation (transforming Gn into G) that takes place over cell wall development. A precise description of the changes in the cellulose structure could not be performed in this study and would require further investigations.

**Acknowledgments:** The authors would like to thank OSEO, Région Bretagne and the French Ministry of Higher Education and Research, for financial support. They would also like to acknowledge the ANR “StressInTrees” (ANR-12-BS09-0004) funded by the French National Research Agency (ANR) and the Russian Foundation for Basic Research (project number 16-14-10256 to TG) for supporting the present study.

**Author Contributions:** O.A., A.B., T.G., and C.B. designed the research. C.G., D.S., A.B., and O.S. performed the experiments. All authors analyzed data. C.G. wrote the manuscript. All authors approved the manuscript.

**Conflicts of Interest:** The authors declare no conflict of interest. The founding partners had no role in the design of the study; in the collection, analyses, or interpretation of data; in the writing of the manuscript; or in the decision to publish the results.

#### References

1. Kvavadze, E.; Bar-Yosef, O.; Belfer-Cohen, A.; Boaretto, E.; Jakeli, N.; Matskevich, Z.; Meshveliani, T. 30,000-year-old wild flax fibers. *Science* **2009**, *325*, 1359. [[CrossRef](#)] [[PubMed](#)]
2. De Bruyne, N.A. Plastic progress. Some further developments in the manufacture and use of synthetic materials for aircraft construction. *Aircr. Eng.* **1939**, *77*–79.
3. Baley, C.; Bourmaud, A. Average tensile properties of French elementary flax fibers. *Mater. Lett.* **2014**, *122*, 159–161. [[CrossRef](#)]
4. Snegireva, A.V.; Ageeva, M.V.; Amenitskii, S.I.; Chernova, T.E.; Ebskamp, M.; Gorshkova, T.A. Intrusive growth of sclerenchyma fibers. *Russ. J. Plant Physiol.* **2010**, *57*, 342–355. [[CrossRef](#)]
5. Mikshina, P.; Chernova, T.; Chemikosova, S.B.; Ibragimova, N.N.; Mokshina, N.; Gorshkova, T.A. Cellulosic fibers: Role of matrix polysaccharides in structure and function. In *Cellulose—Fundamental Aspects*; InTechOpen: Rijeka, Croatia, 2013; pp. 91–112. ISBN 978-953-51-1183-2.
6. Van Dam, J.E.G.; Gorshkova, T.A. Cell walls and Fibers | Fiber formation. In *Encyclopedia of Applied Plant Sciences*; Elsevier: Amsterdam, The Netherlands, 2003; pp. 87–96.
7. Gorshkova, T.A.; Sal'nikov, V.V.; Chemikosova, S.B.; Ageeva, M.V.; Pavlencheva, N.V.; Van Dam, J.E.G. The snap point: A transition point in *Linum usitatissimum* bast fiber development. *Ind. Crop. Prod.* **2003**, *18*, 213–221. [[CrossRef](#)]
8. Bert, F. *Lin Fibre: Culture et Transformation*; Arvalis-Institut du Végétal: Paris, France, 2013; ISBN 9782817901572.
9. Gorshkova, T.; Mokshina, N.; Chernova, T.; Ibragimova, N.; Salnikov, V.; Mikshina, P.; Tryfona, T.; Banasiak, A.; Immerzeel, P.; Dupree, P.; et al. Aspen tension wood fibers contain  $\beta$ -(1→4)-galactans and acidic arabinogalactans retained by cellulose microfibrils in gelatinous walls. *Plant Physiol.* **2015**, *169*, 2048–2063. [[CrossRef](#)] [[PubMed](#)]
10. Arnould, O.; Arinero, R. Towards a better understanding of wood cell wall characterisation with contact resonance atomic force microscopy. *Compos. Part A* **2015**, *74*, 69–76. [[CrossRef](#)]

11. Arnould, O.; Siniscalco, D.; Bourmaud, A.; Le, A.; Baley, C. Better insight into the nano-mechanical properties of flax fibre cell walls. *Ind. Crop. Prod.* **2017**, *97*, 224–228. [[CrossRef](#)]
12. Agarwal, U.P. Raman imaging to investigate ultrastructure and composition of plant cell walls: Distribution of lignin and cellulose in black spruce wood (*Picea mariana*). *Planta* **2006**, *224*, 1141–1153. [[CrossRef](#)] [[PubMed](#)]
13. Himmelsbach, D.S.; Akin, D.E. Near-infrared Fourier-transform Raman spectroscopy of flax (*Linum usitatissimum* L.) stems. *J. Agric. Food Chem.* **1998**, *46*, 991–998. [[CrossRef](#)]
14. Edwards, H.G.M.; Farwell, D.W.; Webster, D. FT Raman microscopy of untreated natural plant fibres. *Spectrochim. Acta Part A Mol. Biomol. Spectrosc.* **1997**, *1425*, 2383–2392. [[CrossRef](#)]
15. Matsko, N.; Mueller, M. AFM of biological material embedded in epoxy resin. *J. Struct. Biol.* **2004**, *146*, 334–343. [[CrossRef](#)] [[PubMed](#)]
16. Meng, Y.; Wang, S.; Cai, Z.; Young, T.M.; Du, G.; Li, Y. A novel sample preparation method to avoid influence of embedding medium during nano-indentation. *Appl. Phys. A* **2013**, *110*, 361–369. [[CrossRef](#)]
17. Konnerth, J.; Harper, D.; Lee, S.H.; Rials, T.G.; Gindl, W. Adhesive penetration of wood cell walls investigated by scanning thermal microscopy (SThM). *Holzforschung* **2008**, *62*, 91–98. [[CrossRef](#)]
18. Wagner, L.; Bader, T.K.; De Borst, K. Nanoindentation of wood cell walls: Effects of sample preparation and indentation protocol. *J. Mater. Sci.* **2014**, *49*, 94–102. [[CrossRef](#)]
19. Clair, B.; Gril, J.; Baba, K.; Thibaut, B.; Sugiyama, J. Precautions for the structural analysis of the gelatinous layer in tension wood. *IAWA J.* **2005**, *26*, 189–195. [[CrossRef](#)]
20. Jäger, A.; Bader, T.; Hofstetter, K.; Eberhardsteiner, J. The relation between indentation modulus, microfibril angle, and elastic properties of wood cell walls. *Compos. Part A Appl. Sci. Manuf.* **2011**, *42*, 677–685. [[CrossRef](#)]
21. Goudenhoft, C.; Bourmaud, A.; Baley, C. Varietal selection of flax over time: Evolution of plant architecture related to influence on the mechanical properties of fibers. *Ind. Crop. Prod.* **2017**, *97*, 56–64. [[CrossRef](#)]
22. Alméras, T.; Clair, B. Critical review on the mechanisms of maturation stress generation in trees. *J. R. Soc. Interface* **2016**, *13*. [[CrossRef](#)] [[PubMed](#)]
23. Roach, M.J.; Mokshina, N.Y.; Badhan, A.; Snegireva, A.V.; Hobson, N.; Deyholos, M.K.; Gorshkova, T.A. Development of Cellulosic Secondary Walls in Flax Fibers Requires  $\beta$ -Galactosidase. *Plant Physiol.* **2011**, *156*, 1351–1363. [[CrossRef](#)] [[PubMed](#)]
24. Gorshkova, T.A.; Chemikosova, S.B.; Sal'nikov, V.V.; Pavlencheva, N.V.; Gur'janov, O.P.; Stolle-Smits, T.; Van Dam, J.E.G. Occurrence of cell-specific galactan is coinciding with bast fiber developmental transition in flax. *Ind. Crop. Prod.* **2004**, *19*, 217–224. [[CrossRef](#)]
25. Jones, L.; Seymour, G.B.; Knox, J.P. Localization of Pectic Galactan in Tomato Cell Walls Using a Monoclonal Antibody Specific to (1/4)- $\beta$ -D-Galactan. *Plant Physiol.* **1997**, *113*, 1405–1412. [[CrossRef](#)] [[PubMed](#)]
26. Tanguy, M.; Bourmaud, A.; Baley, C. Plant cell walls to reinforce composite materials: Relationship between nanoindentation and tensile modulus. *Mater. Lett.* **2016**, *167*, 161–164. [[CrossRef](#)]
27. Christophe, F.; Séné, B.; Mccann, M.C.; Wilson, R.H.; Crinter, R. Fourier-Transform Raman and Fourier-Transform Infrared Spectroscopy. *Plant Physiol.* **1994**, *106*, 1623–1631. [[CrossRef](#)]
28. Gierlinger, N. New insights into plant cell walls by vibrational microspectroscopy. *Appl. Spectrosc. Rev.* **2017**, *4928*, 1–35. [[CrossRef](#)]

